frontiers | Frontiers in Physics

TYPE Mini Review
PUBLISHED 13 October 2025
DOI 10.3389/fphy.2025.1705908

OPEN ACCESS

EDITED BY
Xi Xia,
Shanghai Jiao Tong University, China

REVIEWED BY
Xuesong Li,
Shanghai Jiao Tong University, China
Yanzhi Zhang,
Dalian University of Technology, China

*CORRESPONDENCE
Zhixia He,
zxhe@ujs.edu.cn

RECEIVED 15 September 2025
ACCEPTED 30 September 2025
PUBLISHED 13 October 2025

CITATION
Zhao Y, Huang Y, He Z and Zhong W (2025) Mini-review: air-assisted spray nozzles and applications.
Front. Phys. 13:1705908.
doi: 10.3389/fphy.2025.1705908

Mini-review: air-assisted spray nozzles and applications

Yuanfeng Zhao[1], Yunlong Huang[2], Zhixia He[1]* and Wenjun Zhong[3]

[1]Institute for Energy Research, Jiangsu University, Zhenjiang, China, [2]Rong Tong Aero Engine Technology Corporation Limited, Nanjing, China, [3]School of Energy and Power Engineering, Jiangsu University, Zhenjiang, China

This mini-review summarizes the fundamental principle, spray phenomena, and atomization mechanism of air-assisted spray nozzles, and applications in various aerospace propulsion systems, agriculture irrigation, and some promising areas. The structural configurations and atomization mechanisms of air-assisted nozzles are first introduced, followed by an analysis of key design parameters and their influence on atomization performance. The air-assisted atomization process is further characterized through typical flow regimes, vortex identification techniques, and integrated experimental–numerical approaches. Current practical applications are reviewed, along with potential optimization strategies for nozzle design. Future development directions should emphasize integration with smart agriculture technologies to address emerging demands and challenges in agricultural irrigation and atomization systems.

KEYWORDS

air-assisted injector, atomization, nozzle design, droplet size, vortex dynamics

1 Introduction

Air-assisted spray nozzles adopt the strong interactions and aerodynamic forces [1–4] at the gas-liquid interface to enhance the disruption and atomization of the liquid fuel. It has been widely used in various industrial applications, such as aero-engine fuel atomization [1], smart agriculture and precision plant protection [2, 5–8], spray humidification and cooling [9], chemical and food processing [10], and treatment of respiratory diseases [11].

Conventional liquid jet direct injection and atomization, which relies on high-pressure injection of liquids, now faces many application challenges [12–16]. Liquid jets undergo the primarily breakup due to Rayleigh–Taylor and Kelvin–Helmholtz instabilities, and the secondary breakup influenced by aerodynamic forces under turbulent environment. High-quality atomization typically necessitates elevated injection pressures. In contrast, air-assisted atomization technology shows multiple atomization advantages under low-pressure injection conditions, with the core being the use of the kinetic energy of high-speed gas flow rather than the pressure energy of the liquid to break the liquid, and the spray characteristics can be flexibly controlled by adjusting the gas-liquid ratio and nozzle structure [17–20].

Air-assisted spray differs fundamentally from conventional single-jet atomization in both energy source and breakup mechanism: the former enhances shear-induced instability via gas–liquid interaction, while the latter relies primarily on liquid jet instability driven by high liquid kinetic energy. Although the breakup mechanisms of jets in stationary environments have been extensively studied [21–24],the interaction between high-speed gas flow and liquid jets during air-assisted atomization remains more complex and less understood.

The present mini-review mainly focused on the spray phenomena and breakup mechanisms of air-assisted spray nozzles in Section 2 and applications in combustion engines, agriculture irrigation, and some promising areas in Section 3, followed by the conclusion remarking and suggestions for future directions in Section 4.

2 Schematic and spray phenomena of air-assisted spray nozzles

2.1 Schematic and main geometric parameters

Air-assisted nozzles belong to the category of twin-fluid atomizers, characterized by the introduction of high-speed air during liquid ejection to promote efficient atomization via enhanced shear and interfacial instability. The process involves multiple hydrodynamic mechanisms—including Rayleigh–Taylor instability, Kelvin–Helmholtz instability, boundary-layer stripping, and liquid sheet perforation—with the dominant mechanism varying according to nozzle structure, gas-to-liquid velocity ratio, and operating pressure. Air-assisted atomization centers on intense momentum exchange between high-speed air and the liquid phase, accompanied by interfacial instability-driven fragmentation, typically comprising primary and secondary atomization stages. Such nozzles generally consist of liquid and gas passages along with a mixing chamber. Common configurations include internal-mixing and external-mixing types. Based on the gas–liquid mixing location, air-assisted atomization technology can be categorized into internal-mixing and external-mixing types.

As illustrated in Figure 1a, internal-mixing nozzles achieve gas–liquid mixing within the nozzle, often producing finer droplets but being susceptible to clogging. Nozzle performance is governed by geometric, operational, and performance parameters. Geometric parameters—such as liquid and gas orifice diameters, mixing chamber configuration, and gas–liquid impingement angle—determine the fundamental atomization process and efficiency. Among operational parameters, the gas-to-liquid mass flow ratio (GLR) is a critical variable directly influencing atomization energy and droplet size. Gas and liquid pressures and flow rates must be coordinately regulated to optimize performance. Key performance metrics include the Sauter mean diameter (SMD), droplet size distribution span, and spray cone angle [4, 25–27], which collectively reflect the fineness, uniformity, and spatial distribution of the spray.

External-mixing nozzles, as shown in Figure 1b, employ airflow to act directly on the liquid jet or sheet outside the nozzle, offering structural simplicity and greater operational adaptability. Numerous experimental and computational studies have been conducted on various air-assisted nozzle designs [28, 29]. Patel et al. conducted a numerical simulation study on the externally mixed air-assisted electrostatic nozzle for agriculture, while Dai et al. carried out an experimental study on parameters such as droplet size. The primary geometric parameters of external-mix air-assisted nozzles typically include the liquid orifice diameter, air orifice diameter, relative position of the air and liquid outlets, nozzle spacing, and spray angle. In such nozzles, liquid and air interact externally, where momentum exchange occurs to generate droplets, whereas in internal-mix nozzles, gas–liquid mixing and initial breakup take place inside the nozzle. Overall, the external-mix design features a simpler structure and facilitates independent control of air and liquid flow rates, but the droplet size distribution is more susceptible to external airflow conditions. In contrast, the internal-mix configuration enables stronger gas–liquid interaction and finer atomization, though at the cost of greater structural complexity and higher sensitivity to operating conditions.

In agricultural plant protection, external-mixing designs are widely integrated into unmanned aerial vehicles (UAVs) and precision spray systems, enabling low-drift, high-deposition variable-rate application [30]. In external-mixing nozzles, gas interacts with liquid outside the nozzle, where high-speed airflow aerodynamically shears the low-speed liquid jet or sheet. This design offers simplicity, strong anti-clogging capability, and a broad operating range. In aero-engine and gas turbine combustion chambers, internal-mixing nozzles ensure efficient and stable fuel combustion under low-load conditions, though they exhibit greater structural complexity and higher demands for operational stability [2, 31, 32]. Both approaches predominantly utilize gas-phase kinetic energy to drive droplet breakup, substantially reducing liquid pressure requirements.

2.2 Air-assisted atomization phenomena and mechanism

The air-assisted atomization process can be delineated into several distinct stages: liquid enters the nozzle at low pressure and forms an initial jet or sheet through the discharge orifice; high-speed airflow then interacts with the liquid column or film, inducing stretching, oscillation, and gradual breakup under aerodynamic shear; finally, ligaments and larger fragments undergo further disintegration into droplets, forming a spatially distributed spray plume. This process is characterized by sequential fragmentation from macro-scale structures to micro-scale droplets, with dynamics dominated by gas–liquid interaction intensity and interfacial instability. The Air-Assisted Fuel Injector (AAFI) system uniquely stratifies fuel and air within the injector. It is particularly effective in atomizing heavy fuels—which exhibit high viscosity and surface tension—into fine droplets. Figure 1c illustrates the AAFI atomization process: fuel is first metered into a pre-mixing chamber containing compressed air, where primary atomization occurs via air–fuel interaction; the mixture is then discharged through an annular air nozzle into the combustion chamber, where secondary atomization is enhanced by high-velocity airflow, improving fuel dispersion.

In the field of internal combustion engines, atomization mechanisms—particularly fuel jet breakup, droplet size distribution, and combustion characteristics—have been extensively investigated [21–24]. In contrast, research in agricultural engineering remains relatively limited, often focusing on applied aspects such as spray quality and crop deposition efficacy [25–27]. Although both domains share underlying hydrodynamic principles, performance varies significantly across scales, with jet size effects exert considerable influence on droplet formation and dispersion characteristics. These distinctions underscore the importance of cross-disciplinary mechanistic comparisons and experimental studies for optimizing agricultural spray technologies [28–30].

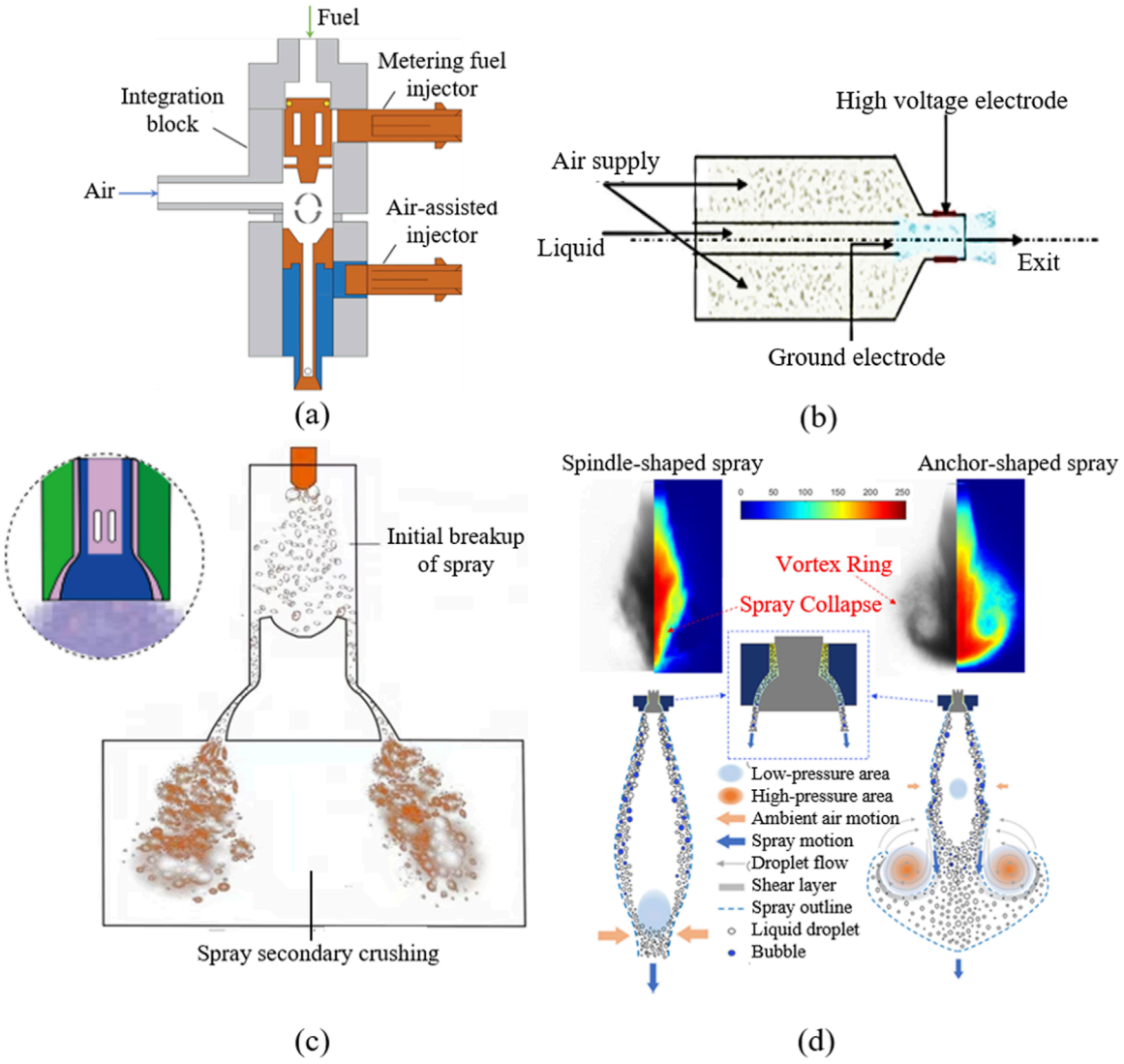

FIGURE 1
Schematic of air-assisted nozzle structure and atomization phenomenon. **(a)** Structure of internal-mixing air-assisted nozzle; **(b)** structure of external-mixing air-assisted nozzle (adapted with permission from [28] Copyright 2017, by Elsevier Ltd.), **(c)** AAFI atomization process (adapted with permission from [33] Copyright 2024, The Authors). **(d)** Different forms of air-assisted spray morphology models for the spindle-shaped spray. (adapted with permission from [34] Copyright 2020, by Elsevier Ltd.).

Furthermore, air-assisted atomization in agriculture is evolving toward intelligent systems incorporating variable-rate spraying and target recognition, presenting new challenges related to droplet size distribution and spray penetration. Systematic research on atomization mechanisms, key influencing factors, and modeling techniques is therefore essential for enhancing combustion efficiency, spray accuracy, and the design of optimized spraying equipment with cross-domain applicability [2, 31–34].

2.3 Effects of vortex formation on air-assisted atomization

Wu et al. [34] experimentally identified two distinct spray patterns of AAFI as illustrated in Figure 1d: the spindle-shaped spray and anchor-shaped spray. Spindle-shaped sprays typically occur with moderate back pressure, and a balanced air–fuel momentum exchange, resulting in elongated and symmetric sprays. In contrast, anchor-shaped sprays often appear under higher back pressure, where strong recirculation zones anchor the spray root, enhancing fuel–air mixing but potentially causing atomization instability. Furthermore, the nozzle structure also exerts a certain influence on the spray pattern. Both patterns exhibit similar near-field spray structures. The key distinction manifests in far-field spray tip morphology. The spindle-shaped spray results from relatively higher injection velocity coupled with intensive droplet breakup and evaporation, which induces low-pressure zones at the spray leading edge and ultimately leads to spray tip collapse. The anchor-type spray is predominantly governed by its leading-edge dual-vortex-ring structure, which originates from shear layer instability induced

by droplet slippage. The shear layer subsequently propagates along the spray periphery, accumulates near the spray tip, then undergoes lateral displacement before finally swirling back into the spray, evolving into a vortex ring configuration.

The influence of vortices on jet breakup has been widely recognized as a critical factor in atomization processes [35]. Vortex structures generated during jet–air interactions not only enhance shear forces at the gas–liquid interface but also induce strong fluctuations in local velocity and pressure fields, thereby accelerating surface wave growth and liquid ligament formation [36, 37]. Large-scale vortices promote primary breakup by destabilizing the liquid column, while smaller-scale vortical motions contribute to the secondary disintegration of ligaments and droplets, ultimately leading to a finer and more uniform spray [24, 37, 38]. Consequently, the evolution and control of vortex dynamics are considered key mechanisms governing atomization efficiency and spray quality. The above-mentioned formation of these vortex rings creates high-pressure zones on both sides near the vortex core, thereby compressing the liquid spray to form hollow vortex rings. In air-assisted sprays, this phenomenon is more pronounced due to the initial presence of abundant microbubbles that rupture distally, facilitating droplet ejection and vortex ring generation at relatively lower spray velocities. This demonstrates strong coupling between air and liquid phase dynamics [34].

Quantifying vortex strength is therefore essential for understanding and optimizing spray dynamics. Common approaches include the evaluation of vorticity, defined as the curl of the velocity field, which provides a direct measure of local rotational intensity. The magnitude of vorticity, often obtained through particle image velocimetry (PIV) or computational fluid dynamics (CFD), is widely employed to characterize the strength of vortical regions. Circulation, expressed as the line integral of velocity around a closed contour, serves as a global indicator of vortex intensity [35–37]. In addition, advanced identification methods such as the Q-criterion or λ_2-criterion allow for precise recognition and assessment of coherent vortex structures.

Geometric optimization, including the use of swirlers or tailored nozzle exits, can significantly affect vortex strength and stability. Operational parameters, such as the air-to-liquid ratio and injection pressure, provide further control over the flow field. Moreover, the integration of flow-guiding elements or micro-structures enables fine-tuned manipulation of local vortices [39, 40]. In the future, intelligent control systems that couple real-time sensing with dynamic flow adjustment are expected to offer advanced regulation of vortex behavior, thereby achieving superior atomization performance [41].

3 Applications of air-assisted spray nozzles

3.1 Small-scale air-assisted nozzles in energy-related engines

The outlet diameter of Small-scale air-assisted nozzles typically ranges from 1 to 8 mm, and they are capable of spraying droplets with a Sauter Mean Diameter of 5–50 μm [42]. In power engineering applications such as internal combustion engines, research on air-assisted nozzles emphasizes transient fuel jet breakup and combustion efficiency improvement. Advanced diagnostic techniques, including laser-induced fluorescence (LIF) and particle image velocimetry (PIV), are widely employed to investigate the physical properties of air-assisted sprays. These methods enable high-precision visualization and measurement of key parameters such as droplet size, velocity field, and spatial distribution. Phase Doppler particle analyzers (PDPA) and laser diffraction particle sizing instruments are commonly utilized to evaluate atomization performance under varying injection pressures, flow conditions, and nozzle geometries [43–61].

Figure 2a presents an air-assisted direct injection (AADI) system designed to mitigate knock in high-compression-ratio elliptical rotary engine. The AADI system demonstrated effective knock suppression, improved thermal efficiency, and reduced heat transfer losses compared to baseline configurations, highlighting its potential for enhancing anti-knock performance and overall energy efficiency.

3.2 Large-scale air-assisted nozzles in agricultural irrigation

The application of air-assisted atomization in agricultural engineering goes far beyond "spraying", and its core value lies in achieving precise, efficient and environmentally friendly plant protection operations, which are manifested in significantly reducing drift pollution [62–64], improving canopy penetration and uniform deposition [65, 66], adapting to low-volume spraying, and achieving precise variable spraying [67], etc. Large-scale air-assisted nozzles range from 10 to 50 mm [20], generating droplets of 80–450 μm, depending on airflow and liquid properties [18]. A large number of experimental studies using techniques such as laser particle size analyzer, high-speed photography and particle image velocity measurement have revealed the effects of nozzle structure, gas-liquid ratio and spray pressure on droplet size distribution, droplet deposition efficiency and drift behavior [68, 69]. In terms of numerical simulation, Euler-Lagrange coupling, VOF and large eddy simulation (LES) methods are widely used in agricultural engineering to study gas-liquid interactions. The simulation in agricultural engineering focuses on the transport and deposition distribution of droplets in the canopy [2, 65–67, 70].

Air-assisted spray technology has been widely used for pest and disease control in orchard crops [8, 69, 71, 72] and is gradually expanding to areas such as between facility farmers [29, 73–76]. Air-assisted spraying has been widely integrated into a variety of agricultural spraying equipment [77]. Figure 2b presents an air-assisted spraying system specifically engineered for tunnel boring equipment. This system utilizes the Coanda effect to improve atomization performance and increase spray projection distance. By optimizing air and water pressure parameters, the system achieves substantial enhancements in dust suppression efficiency, with total coal dust and respirable dust suppression rates exceeding those of conventional systems by more than 30%.

In recent years, agricultural drones based on air-assisted spraying, orchard air-assisted sprayers [20, 78, 79], high-gap boom sprayers [30, 71] have been widely used, and intelligent devices have been continuously developed, significantly improving the efficiency and uniformity of pesticide application. At the same time, by

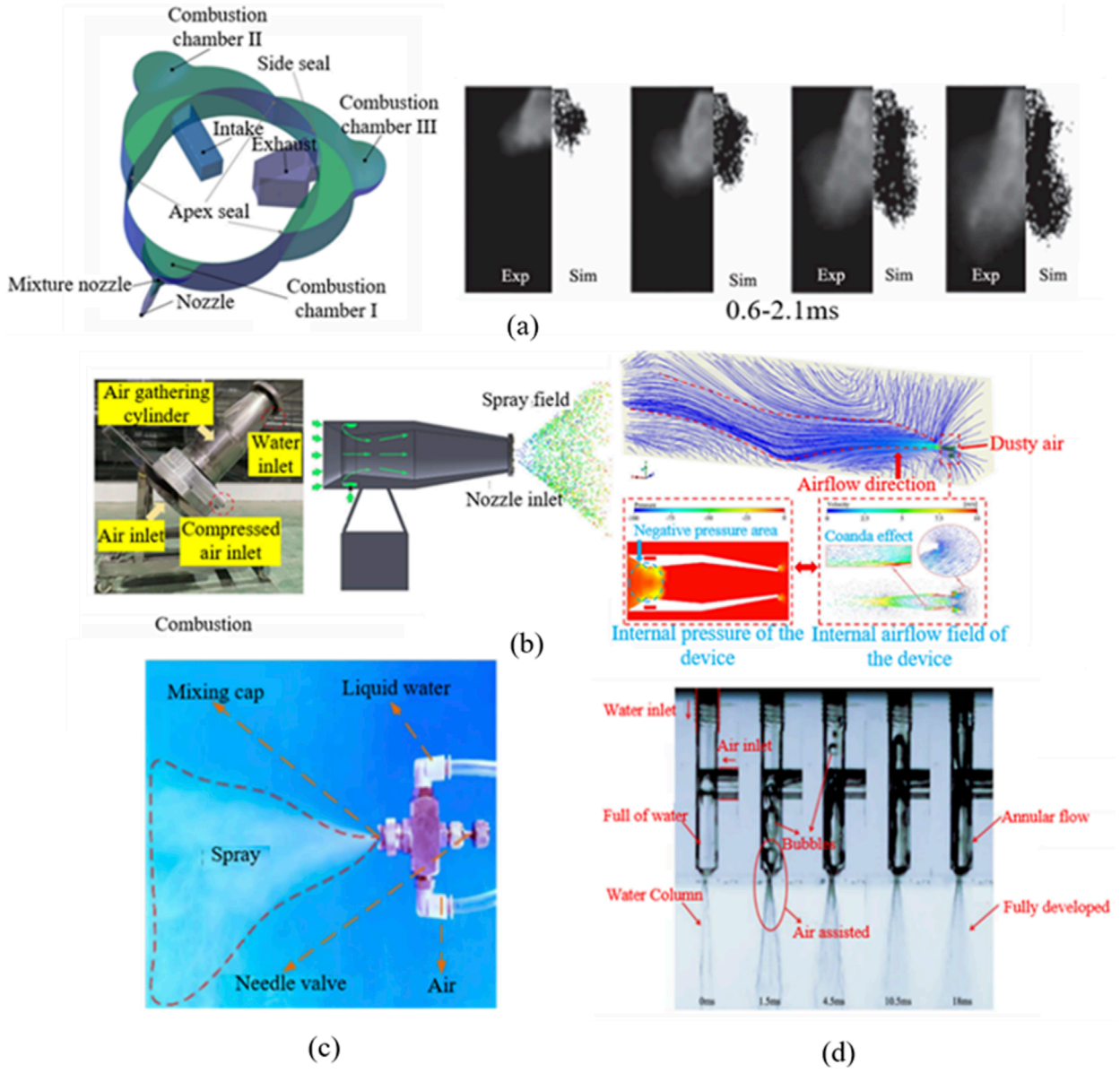

FIGURE 2
Applications of air-assisted nozzles. **(a)** Simulated and experimental spray morphologies at different moments of elliptical rotor engine (adapted with permission from [57]Copyright 2024, by Elsevier Ltd.), **(b)** Air-assisted Spraying Device for Dust Suppression on Tunneling Machine and Vector Diagram of the spray field (adapted with permission from [62]Copyright 2025, by Elsevier Ltd.), **(c)** Air-assisted atomization humidifier (adapted with permission from [63] Copyright 2025, by Elsevier Ltd.), **(d)** Compressed air injects into mixing chamber filled with water, (adapted with permission from [64]Copyright 2023, by Elsevier Ltd.).

combining methods such as CFD simulation [80, 81] and response surface optimization [82], researchers have proposed a variety of improvement schemes in terms of spray Angle, wind speed control, droplet size regulation, etc. [2, 5, 6, 62, 83–85], effectively reducing the risk of pesticide drift and improving pesticide utilization. Some intelligent spray systems also integrate lidar, ultrasonic sensors or machine vision modules [86–90] to achieve real-time perception of crop canopy structure and adaptive control of spray volume, further promoting the development of variable spray and targeted application technology. Also, the integration of unmanned aerial vehicle platforms and air-assisted systems has become a hot application direction [91, 92]. Drones equipped with air-assisted nozzles can achieve uniform atomization and precise control while hovering, showing unique advantages in areas such as mountain orchards that are difficult to cover with traditional machinery. Ahmed et al. [90, 91] noted that although unmanned aerial vehicles have been widely used in crop management, monitoring, seeding and pesticide spraying, they still face many challenges when used as spray platforms. Unlike conventional drones, spray drones need to perform tasks in dynamic payloads and complex environments, which poses higher requirements for real-time obstacle detection, path planning, and collision avoidance capabilities.

3.3 Future designs for air-assisted nozzles

In recent years, machine learning and intelligent optimization algorithms have provided new ideas for nozzle design [90, 91]. On the one hand, machine learning models based on experimental data and numerical simulation results (such as random forests, support vector machines, deep neural networks) can quickly predict spray particle size distribution, spray Angle and deposition effect, significantly reducing the experimental costs required for the development of traditional nozzles [63, 82, 93]. On the other hand, methods such as genetic algorithms, multi-objective optimization, and reinforcement learning have been applied to nozzle structure and flow field design to achieve comprehensive optimization of nozzle geometry, gas-liquid ratio, and gas flow path [94, 95].

Air-assisted atomization technology has been successfully implemented in the refrigeration industry. Figure 2c presents the Air-Assisted Atomization and Humidification (AAAH) technology designed to address humidification and cooling challenges in high-power fuel cell systems. The results indicate that AAAH significantly enhances the cathode inlet relative humidity and water recovery rate while reducing thermal load. Figure 2d investigates the sensitivity of air-assisted atomizers in outdoor snowmakers under varying operational conditions. The findings reveal that the spray cone angle initially increases and then decreases with rising air-to-water pressure ratio, while the Sauter Mean Diameter (SMD) continuously declines. Additionally, the study demonstrates that atomizers employing an independent air-water injection mode effectively prevent clogging and improve flow capacity.

4 Discussions and concluding remarks

Air-assisted atomizing nozzles demonstrate broad application potential in agricultural and power engineering due to their ability to achieve efficient atomization under low-pressure conditions. However, several key scientific challenges remain in nozzle optimization design. Central among these is a deeper understanding of atomization mechanisms, particularly the role of high-speed gas flow in perturbing and disrupting the liquid jet interface. While jet instability in stationary environments has been well studied, the interaction between high-speed gas flow and liquid jets in air-assisted nozzles remains more complex and less understood. The characteristics of vortex dynamics and their effects on droplet size distribution, spray uniformity, and drift behavior have not been fully elucidated, impeding scientifically guided nozzle optimization and flow field control. Future research should prioritize integrated experimental and numerical approaches to unravel the multi-scale mechanisms of gas–liquid interaction, which will be crucial for advancing nozzle design and application.

Additive manufacturing, such as 3D printing, enables the fabrication of complex internal geometries and microstructures that are difficult to achieve with conventional machining, thereby improving air–liquid mixing efficiency and spray performance [96, 97]. It also allows for rapid prototyping and customization, accelerating design iteration while reducing costs. In parallel, lightweight composite materials, including carbon fiber and ceramic-based composites, provide significant advantages in terms of weight reduction, durability, and resistance to wear and corrosion. Moreover, functional enhancements such as hydrophobicity or self-cleaning surfaces can be integrated through advanced material processing [98].

Looking forward, the evolution of smart agriculture imposes increasing demands on spray and atomization technologies. Enhancing pesticide and water use efficiency is essential to achieve precise chemical application and water-saving irrigation. Concurrently, controlling spray drift, ensuring environmental safety, and adapting to complex field wind conditions present ongoing challenges. Air-assisted atomizing nozzles must balance fine droplet generation with anti-drift performance and target deposition efficiency. Future developments should emphasize integration with smart sensing, machine learning, and automatic control technologies to enable dynamic, adaptive regulation of spraying systems.

Author contributions

YZ: Writing – original draft, Investigation. YH: Writing – review and editing, Investigation. ZH: Writing – review and editing, Conceptualization, Supervision. WZ: Writing – review and editing, Resources.

Funding

The author(s) declare that financial support was received for the research and/or publication of this article. National Natural Science Foundation of China (No.52376113).

Conflict of interest

Author YH was employed by Rong Tong Aero Engine Technology Corporation Limited.

The remaining authors declare that the research was conducted in the absence of any commercial or financial relationships that could be construed as a potential conflict of interest.

Generative AI statement

The author(s) declare that no Generative AI was used in the creation of this manuscript.

Any alternative text (alt text) provided alongside figures in this article has been generated by Frontiers with the support of artificial intelligence and reasonable efforts have been made to ensure accuracy, including review by the authors wherever possible. If you identify any issues, please contact us.

Publisher's note

References

1. Wu H, Wang L, Wu Y, Sun B, Zhao Z, Liu F. Spray performance of air-assisted kerosene injection in a constant volume chamber under various in-cylinder GDI engine conditions. *Appl Therm Eng* (2019) 150:762–9. doi:10.1016/j.applthermaleng.2019.01.014

2. Wang G, Liu M, Ou M, Jia W, Jiang L, Li Z, et al. Anti-drift performance of a hoods spray system for soybean (Glycine max (L.) Merr.)-maize (Zea mays L.) strip intercropping. *Crop Prot* (2024) 181:106689. doi:10.1016/j.cropro.2024.106689

3. Xie H, Song L, Xie Y, Pi D, Shao C, Lin Q. An experimental study on the macroscopic spray characteristics of biodiesel and diesel in a constant volume chamber. *Energies* (2015) 8(6):5952–72. doi:10.3390/en8065952

4. Hyungsuk K, Chun T. *Demonstration of air-power-assist engine technology for clean combustion and direct energy recovery in heavy duty application*. Office of Scientific and Technical Information Technical Reports (2008).

5. Wu J, Yang S, Gao Y, Pan X, Zou W, Wei Y, et al. Optimization of a boom height ultrasonic detecting model for the whole growth cycle of wheat: affected by the oscillation of the three-section boom of the sprayer. *Agriculture* (2024) 14(10):1733. doi:10.3390/agriculture14101733

6. Xi T, Li C, Qiu W, Wang H, Lv X, Han C, et al. Droplet deposition behavior on a pear leaf surface under wind-induced vibration. *Appl Eng Agric* (2020) 36(6):913–26. doi:10.13031/aea.14031

7. Zhu Q, Zhu Z, Zhang H, Gao Y, Chen L. Design of an electronically controlled fertilization system for an air-assisted side-deep fertilization machine. *Agriculture* (2023) 13(12):2210. doi:10.3390/agriculture13122210

8. Hussain Tunio M, Gao J, Ahmed QW, Ali SS, Chen J, Ali Chandio F, et al. Effects of droplet size and spray interval on root-to-shoot ratio, photosynthesis efficiency, and nutritional quality of aeroponically grown butterhead lettuce. *Int J Agric Biol Eng* (2022) 15(1):79–88. doi:10.25165/j.ijabe.20221501.6725

9. Liu H, Yang C, Xie R, Zhang Y, Li R, Chen Y, et al. High-pressure air cooling-assisted friction rolling additive manufacturing: an effective approach for optimizing microstructure and mechanical properties of Al-Zn-Mg-Cu alloy. *Mater Sci Eng A* (2025) 942:148701. doi:10.1016/j.msea.2025.148701

10. Wang L, Huang T, Cao HX, Yuan QX, Liang ZP, Liang GX. Application of air-assisted liquid-liquid microextraction for determination of some fluoroquinolones in milk powder and egg samples: Comparison with conventional dispersive liquid-liquid microextraction. *Food Anal Methods* (2016) 9(8):2223–30. doi:10.1007/s12161-016-0409-6

11. Guo G, Zhang L, Li T, Li C, Zhang Y, Ren H, et al. A new exhalation-assisted aerosol delivery method for nasal administration. *Powder Technol* (2023) 427:118708. doi:10.1016/j.powtec.2023.118708

12. Ferreira S, Nicoletti VR. Complex coacervation assisted by a two-fluid nozzle for microencapsulation of ginger oil: effect of atomization parameters. *Food Res Int* (2020) 138:109828. doi:10.1016/j.foodres.2020.109828

13. Nuyttens D, Baetens K, De Schampheleire M, Sonck B. Effect of nozzle type, size and pressure on spray droplet characteristics. *Biosyst Eng* (2007) 97(3):333–45. doi:10.1016/j.biosystemseng.2007.03.001

14. Copan J, Balachandar R, Berruti F. Droplet size-velocity characteristics of sprays generated by two-phase feed nozzles. *Chem Eng Commun* (2007) 184(1):105–24. doi:10.1080/00986440108912843

15. Li M, Yang H, Wang J, Li G, Tang J. An experimental investigation of the impact of surface tension and viscosity on the atomization effect of a solid cone nozzle. *Appl Sci* (2023) 13(7):4522. doi:10.3390/app13074522

16. Ulrich H, Lehnert B, Guénot D, Svendsen K, Lundh O, Wensing M, et al. Effects of liquid properties on atomization and spray characteristics studied by planar two-photon fluorescence. *Phys Fluids* (2022) 34(8):083305. doi:10.1063/5.0098922

17. Wei Z, Li R, Xue X, Sun Y, Zhang S, Li Q, et al. Research status, methods and prospects of air-assisted spray technology. *Agron* (2023) 13(5):1407. doi:10.3390/agronomy13051407

18. Wandkar SV, Mathur SM, Dhande KG, Jadhav PP, Gholap BS. Air assisted sprayer for improved spray penetration in greenhouse floriculture crops. *J The Inst Eng (India) Ser A* (2015) 96(1):1–9. doi:10.1007/s40030-015-0112-4

19. Jiang Y, Yang Z, Xu X, Shen D, Jiang T, Xie B, et al. Wetting and deposition characteristics of air-assisted spray droplet on large broad-leaved crop canopy. *Front Plant Sci* (2023) 14:1079703. doi:10.3389/fpls.2023.1079703

20. Pan X, Yang S, Gao Y, Wang Z, Zhai C, Qiu W. Evaluation of spray drift from an electric boom sprayer: impact of boom height and nozzle type. *Agron* (2025) 15(1):160. doi:10.3390/agronomy15010160

21. Jeon DS, Kim NI. Improved stabilization mechanisms of CH4+H2 lifted flames using laminar non-premixed jets with fuel dilution. *Int J Hydrogen Energ* (2025) 162:150763. doi:10.1016/j.ijhydene.2025.150763

22. Jung WH, Park HS. New melt jet breakup length model considering the boiling effect under fuel–coolant interaction. *Appl Therm Eng* (2025) 280:128187. doi:10.1016/j.applthermaleng.2025.128187

23. Li H, Jia M, Ding R, Li X, Zhang Z, Zhang Y. An improved Kelvin-Helmholtz Rayleigh-Taylor (KH-RT) breakup model with wide fuel applicability based on data-driven techniques. *Energy* (2025) 334:137661. doi:10.1016/j.energy.2025.137661

24. Zhang T, Wang W, Li Z, Zhang H, Wei H, Li R, et al. Numerical simulation of the primary breakup of fuel jet with incoming positive velocity gradient. *Green Energ Resour* (2024) 2(3):100090. doi:10.1016/j.gerr.2024.100090

25. Li G, Chen L, Li L, Yi T, Ding C, Wang J, et al. Modeling and experimental validation of the atomization efficiency of a rotary atomizer for aerial spraying. *Agron* (2022) 12(2):419. doi:10.3390/agronomy12020419

26. Mopuri L, Grahn V, Sedarsky D, Hyvönen J. Shape/penetration analysis and comparisons of isolated spray plumes in a multi-hole diesel spray. *Exp Fluids* (2024) 65(6):92. doi:10.1007/s00348-024-03829-6

27. Abraheem SN, Alheidary MH. Evaluation of spray droplets characteristics depending on the configuration of boomless nozzle. *IOP Conf Ser Earth Environ Sci* (2022) 1060(1):012128. doi:10.1088/1755-1315/1060/1/012128

28. Patel MK, Praveen B, Sahoo HK, Patel B, Kumar A, Singh M, et al. An advance air-induced air-assisted electrostatic nozzle with enhanced performance. *Comput Electron Agric* (2017) 135:280–8. doi:10.1016/j.compag.2017.02.010

29. Dai S, Zhang J, Jia W, Ou M, Zhou H, Dong X, et al. Experimental study on the droplet size and charge-to-mass ratio of an air-assisted electrostatic nozzle. *Agriculture* (2022) 12(6):889. doi:10.3390/agriculture12060889

30. Cui L, Xue X, Le F, Mao H, Ding S. Design and experiment of electro hydraulic active suspension for controlling the rolling motion of spray boom. *Int J Agric Biol Eng* (2019) 12(4):72–81. doi:10.25165/j.ijabe.20191204.4648

31. Chang H, Yang Z, Tu Z. Experimental study on the cold-start performance of a gas heating assisted air-cooled proton exchange membrane fuel cell stack. *Renew Energ* (2024) 234:121224. doi:10.1016/j.renene.2024.121224

32. Ma X, Li F, Wang S. Droplet velocity and size characteristics of biodiesel in an air-assisted pressure swirl atomizer during industrial furnace. *Fuel* (2025) 388:134446. doi:10.1016/j.fuel.2025.134446

33. Wang D, Yin P, Lei J, Deng X, Jiia D, Ouyang Q, et al. Research overview of air-assisted injection technology for aviation heavy fuel. *J Aerospace Power* (2024) 40:20240500. doi:10.13224/j.cnki.jasp.20240500

34. Wu H, Zhang F, Zhang Z, Guo Z, Zhang W, Gao H. On the role of vortex-ring formation in influencing air-assisted spray characteristics of n-heptane. *FUEL* (2020) 266:117044. doi:10.1016/j.fuel.2020.117044

35. Cao T, He Z, Zhou H, Guan W, Zhang L, Wang Q. Experimental study on the effect of vortex cavitation in scaled-up diesel injector nozzles and spray characteristics. *Exp Therm Fluid Sci* (2020) 113:110016. doi:10.1016/j.expthermflusci.2019.110016

36. Guo G, Lu K, Xu S, Yuan J, Bai T, Yang K, et al. Effects of in-nozzle liquid fuel vortex cavitation on characteristics of flow and spray: numerical research. *Int Commun Heat Mass Transfer* (2023) 148:107040. doi:10.1016/j.icheatmasstransfer.2023.107040

37. Tang Y, Wang P, Liu Y. Phase-locking PIV measurement of vortex–vortex interactions inside dual-slit cavity during high-intensity acoustic modulation. *Exp Therm Fluid Sci* (2025) 166:111483. doi:10.1016/j.expthermflusci.2025.111483

38. Liu W, Tang J, Lu Y, Xie C, Liu Q, Lee C-F. Eulerian–Lagrangian modeling of spray G atomization with focus on vortex evolution and its interaction with cavitation. *Appl Math Modell* (2022) 107:103–32. doi:10.1016/j.apm.2022.01.017

39. Zhang Y, He X. Influence of air-assisted atomizer structure on ignition and flame propagation in a trapped-vortex cavity. *Case Stud Therm Eng* (2022) 39:102416. doi:10.1016/j.csite.2022.102416

40. García JA, Santolaya JL, Lozano A, Barreras F, Calvo E. Experimental characterization of the viscous liquid sprays generated by a Venturi-vortex atomizer. *Chem Eng Process* (2016) 105:117–24. doi:10.1016/j.cep.2016.01.004

41. Budhraja N, Pal A, Mishra RS. Vortex flow plasma reforming for hydrogen production from atomized water-methanol mixture and parameter optimization using RSM and ANN-GA. *Renew Energ* (2025) 247:123026. doi:10.1016/j.renene.2025.123026

42. Wu H, Zhang F, Zhang Z. Fundamental spray characteristics of air-assisted injection system using aviation kerosene. *Fuel* (2021) 286:119420. doi:10.1016/j.fuel.2020.119420

43. Jin SH, Brear M, Watson H, Brewster S. An experimental study of the spray from an air-assisted direct fuel injector. *P MECH ENG D-j AUT* (2008) 222(10):1883–94. doi:10.1243/09544070jauto710

44. Boretti AA, Jin SH, Zakis G, Brear MJ, Attard W, Watson H, et al. *Experimental and numerical study of an air assisted fuel injector for a D.I.S.I. engine*. Warrendale, PA: SAE Technical Paper Series (2007).

45. Hu J, Liu B, Zhang C, Gao H, Zhao Z, Zhang F, et al. Experimental study on the spray characteristics of an air-assisted fuel injection system using kerosene and gasoline. *Fuel* (2019) 235:782–94. doi:10.1016/j.fuel.2018.08.083

46. Vigo-Morancho A, Videgain M, Boné A, Vidal M, Javier García-Ramos F. Static and dynamic study of the airflow behavior generated by two air assisted

sprayers commonly used in 3D crops. *Comput Electron Agric* (2024) 216:108535. doi:10.1016/j.compag.2023.108535

47. Gavali PB, Kalashetty SS. Experimental analysis of spray droplet deposition behaviour for centrifugal assisted spinning disc sprayer. *Mater Today Proc* (2023) 92:258–63. doi:10.1016/j.matpr.2023.04.518

48. Cheraiet A, Codis S, Lienard A, Vergès A, Carra M, Bastidon D, et al. EvaSprayViti: a flexible test bench for comparative assessment of the 3D deposition efficiency of vineyard sprayers at multiple growth stages. *Biosyst Eng* (2024) 241:1–14. doi:10.1016/j.biosystemseng.2024.03.008

49. Li Y, Wang X, Zhang Z, Liang J, Sun H, Li J. Design and test investigation of a 3WZ-600 profiling sprayer for dwarf-dense planting jujube orchard. *Biosyst Eng* (2025) 250:213–24. doi:10.1016/j.biosystemseng.2024.12.015

50. Khodabakhshian KR, Seyyed Ali Bik Lavasani HS, Javadpour SM. Investigating the effect of installing an electrostatic system on the performance of an orchard automizer sprayer. *J Electrostat* (2025) 136:104122. doi:10.1016/j.elstat.2025.104122

51. Boretti A, Jin SH, Brear M, Zakis G, Attard W, Watson H, et al. Experimental and numerical study of a spark ignition engine with air-assisted direct injection. *P MECH ENG D-j AUT* (2008) 222(6):1103–19. doi:10.1243/09544070jauto712

52. Du B, Zhao Z. Numerical prediction of the spray from an air-assisted fuel injection system via Eulerian–Lagrangian approach. *Energy Rep* (2021) 7:6718–32. doi:10.1016/j.egyr.2021.09.128

53. Chen Z, Liao B, Yu Y, Qin T. Effect of equivalence ratio on spark ignition combustion of an air-assisted direct injection heavy-fuel two-stroke engine. *Fuel* (2022) 313:122646. doi:10.1016/j.fuel.2021.122646

54. Zhao J, Fu L, Ding H, Bai B, Zhang D, Liu J, et al. Numerical simulation of working process and gas-liquid interaction mechanism of air assisted nozzle. *Int J Multiphase Flow* (2023) 164:104453. doi:10.1016/j.ijmultiphaseflow.2023.104453

55. Zhao J, Ding H, Fu L, Bai B, Zhang D, Liu J, et al. Energy analysis and research on injection control parameter influence mechanism of air assisted spray system. *Fuel* (2023) 346:128204. doi:10.1016/j.fuel.2023.128204

56. Liao B, Zhang F, Chen Z, Qin T, Lin X, Guo Y. Effect of injection strategy on an air-assisted direct injection aviation kerosene two-stroke engine. *Appl Therm Eng* (2023) 233:121193. doi:10.1016/j.applthermaleng.2023.121193

57. Lin X, Liao B, Guo Y, Qin T, Zhu H, Chen Z. Impact on air-assisted direct injection on knock and energy conversion in a downsized elliptical rotary engine with high compression ratio. *Appl Therm Eng* (2024) 253:123704. doi:10.1016/j.applthermaleng.2024.123704

58. Liao B, Zhang F, Qin T, Guo Y, Lin X, Chen Z. Numerical study on the effect of air-assisted nozzle shape on kerosene spray and flow characteristics. *Aerosp Sci Technol* (2024) 154:109488. doi:10.1016/j.ast.2024.109488

59. Kira O, Dubowski Y, Linker R. *In-situ* open path FTIR measurements of the vertical profile of spray drift from air-assisted sprayers. *Biosyst Eng* (2018) 169:32–41. doi:10.1016/j.biosystemseng.2018.01.010

60. Kaliniewicz Z, Lipiński A, Markowski P, Szczyglak P, Lipiński S. The influence of selected operating parameters of a field sprayer on boom stability. *Comput Electron Agric* (2024) 219:108787. doi:10.1016/j.compag.2024.108787

61. Salas B, Salcedo R, Ortega P, Grella M, Gil E. Use of ultrasound anemometers to study the influence of air currents generated by a sprayer with an electronic control airflow system on foliar coverage. Effect of droplet size. *Comput Electron Agric* (2022) 202:107381. doi:10.1016/j.compag.2022.107381

62. Delele MA, Jaeken P, Debaer C, Baetens K, Endalew AM, Ramon H, et al. CFD prototyping of an air-assisted orchard sprayer aimed at drift reduction. *Comput Electron Agric* (2007) 55(1):16–27. doi:10.1016/j.compag.2006.11.002

63. Herkins MJ, Hong S-W, Zhao L, Zhu H, Jeon H. Computer simulation of pesticide deposition and drift by conventional and intelligent air-assisted sprayers in apple orchards. *Smart Agric Technology* (2025) 12:101111. doi:10.1016/j.atech.2025.101111

64. Wu S, Liu J, Wang J, Hao D, Wang R. The motion of strawberry leaves in an air-assisted spray field and its influence on droplet deposition. *Trans ASABE* (2021) 64(1):83–93. doi:10.13031/trans.14143

65. Guo J, Dong X, Qiu B. Analysis of the factors affecting the deposition coverage of air-assisted electrostatic spray on tomato leaves. *Agron* (2024) 14(6):1108. doi:10.3390/agronomy14061108

66. Lin J, Cai J, Xiao L, Liu K, Chen J, Ma J, et al. An angle correction method based on the influence of angle and travel speed on deposition in the air-assisted spray. *Crop Prot* (2024) 175:106444. doi:10.1016/j.cropro.2023.106444

67. Khot LR, Ehsani R, Albrigo G, Larbi PA, Landers A, Campoy J, et al. Air-assisted sprayer adapted for precision horticulture: spray patterns and deposition assessments in small-sized citrus canopies. *Biosyst Eng* (2012) 113(1):76–85. doi:10.1016/j.biosystemseng.2012.06.008

68. Wang G, Dong X, Jia W, Ou M, Yu P, Wu M, et al. Influence of wind speed on the motion characteristics of peach leaves (Prunus persica). *Agriculture* (2024) 14(12):2307. doi:10.3390/agriculture14122307

69. Cui L, Mao H, Xue X, Ding S, Qiao B. Design optimization and test for a pendulum suspension of the crop sprayer boom in dynamic conditions based on a six DOF motion simulator. *Int J Agric Biol Eng* (2018) 11(3):76–85. doi:10.25165/j.ijabe.20181103.3717

70. Zhou Q, Xue X, Chen C, Cai C, Jiao Y. Canopy deposition characteristics of different orchard pesticide dose models. *Int J Agric Biol Eng* (2023) 16(3):1–6. doi:10.25165/j.ijabe.20231603.7665

71. Tunio MH, Gao J, Lakhiar IA, Solangi KA, Qureshi WA, Shaikh SA, et al. Influence of atomization nozzles and spraying intervals on growth, biomass yield, and nutrient uptake of butter-head lettuce under aeroponics system. *Agron* (2021) 11(1):97. doi:10.3390/agronomy11010097

72. Lin J, Ma J, Liu K, Huang X, Xiao L, Ahmed S, et al. Development and test of an autonomous air-assisted sprayer based on single hanging track for solar greenhouse. *Crop Prot* (2021) 142:105502. doi:10.1016/j.cropro.2020.105502

73. Gao J, Guo Y, Hussain Tunio M, Chen X, Chen Z. Design of a high-voltage electrostatic ultrasonic atomization nozzle and its droplet adhesion effects on aeroponically cultivated plant roots. *Int J Agric Biol Eng* (2023) 16(2):30–7. doi:10.25165/j.ijabe.20231602.7222

74. Hu Y, Chen Y, Wei W, Hu Z, Li P. Optimization design of spray cooling fan based on CFD simulation and field experiment for horticultural crops. *Agriculture* (2021) 11(6):566. doi:10.3390/agriculture11060566

75. Liu Z, Chen J, Guo J, Qiu B. Numerical simulation and validation of droplet deposition on tomato leaf surface under air-assisted spraying. *Agron* (2024) 14(8):1661. doi:10.3390/agronomy14081661

76. Lin J, Cai J, Ouyang J, Xiao L, Qiu B. The influence of electrostatic spraying with waist-shaped charging devices on the distribution of long-range air-assisted spray in greenhouses. *Agron* (2024) 14(10):2278. doi:10.3390/agronomy14102278

77. Jing L, Wei X. Spray deposition and distribution on rice as affected by a boom sprayer with a canopy-opening device. *Agriculture* (2022) 13(1):94. doi:10.3390/agriculture13010094

78. Ou M, Zhang Y, Wu M, Wang C, Dai S, Wang M, et al. Development and experiment of an air-assisted sprayer for vineyard pesticide application. *Agriculture* (2024) 14(12):2279. doi:10.3390/agriculture14122279

79. Ahmed S, Qiu B, Kong C-W, Xin H, Ahmad F, Lin J. A data-driven dynamic obstacle avoidance method for liquid-carrying plant protection UAVs. *Agron* (2022) 12(4):873. doi:10.3390/agronomy12040873

80. Yan C, Niu C, Ma S, Tan H, Xu L. CFD models as a tool to analyze the deformation behavior of grape leaves under an air-assisted sprayer. *Comput Electron Agric* (2022) 198:107112. doi:10.1016/j.compag.2022.107112

81. Salcedo R, Vallet A, Granell R, Garcerá C, Moltó E, Chueca P. Eulerian–Lagrangian model of the behaviour of droplets produced by an air-assisted sprayer in a citrus orchard. *Biosyst Eng* (2017) 154:76–91. doi:10.1016/j.biosystemseng.2016.09.001

82. Mohanty SP, Raheman H. Performance optimization of an air-assisted electrostatic spraying unit using response surface methodology. *J Electrostat* (2024) 131:103963. doi:10.1016/j.elstat.2024.103963

83. Shi N, Chen Z, Li H, Hua H, Xu T, Ye J. Development and assessment of a novel single-drive variable angle spraying machine. *Sci Rep* (2024) 14(1):31264. doi:10.1038/s41598-024-82680-5

84. Ji X, Wang A, Wei X. Precision control of spraying quantity based on linear active disturbance rejection control method. *Agriculture* (2021) 11(8):761. doi:10.3390/agriculture11080761

85. Ou M, Hu T, Hu M, Yang S, Jia W, Wang M, et al. Experiment of canopy leaf area density estimation method based on ultrasonic echo signal. *Agriculture* (2022) 12(10):1569. doi:10.3390/agriculture12101569

86. Liu H, Zhu H. Evaluation of a laser scanning sensor in detection of complex-shaped targets for variable-rate sprayer development. *Trans ASABE* (2016) 59(5):1181–92. doi:10.13031/trans.59.11760

87. Shen Y, Zhu H, Liu H, Chen Y, Ozkan E. Development of a laser-guided, embedded-computer-controlled, air-assisted precision sprayer. *Trans ASABE* (2017) 60(6):1827–38. doi:10.13031/trans.12455

88. Liu J, Abbas I, Noor RS. Development of deep learning-based variable rate agrochemical spraying system for targeted weeds control in strawberry crop. *Agron* (2021) 11(8):1480. doi:10.3390/agronomy11081480

89. Zheng K, Zhao X, Han C, He Y, Zhai C, Zhao C. Design and experiment of an automatic row-oriented spraying system based on machine vision for early-stage maize corps. *Agriculture* (2023) 13(3):691. doi:10.3390/agriculture13030691

90. Ahmed S, Qiu B, Ahmad F, Kong C-W, Xin H. A State-of-the-Art analysis of obstacle avoidance methods from the perspective of an agricultural sprayer UAV's operation scenario. *Agron* (2021) 11(6):1069. doi:10.3390/agronomy11061069

91. Ahmed S, Xin H, Faheem M, Qiu B. Stability analysis of a sprayer UAV with a liquid tank with different outer shapes and inner structures. *Agriculture* (2022) 12(3):379. doi:10.3390/agriculture12030379

92. Ahmad F, Zhang S, Qiu B, Ma J, Xin H, Qiu W, et al. Comparison of water sensitive paper and glass strip sampling approaches to access spray deposit by UAV sprayers. *Agron* (2022) 12(6):1302. doi:10.3390/agronomy12061302

93. Li Y, Yuan J, Liu X, Niu Z, Chen B, Liu X. Spraying strategy optimization with genetic algorithm for autonomous air-assisted sprayer in Chinese heliogreenhouses. *Comput Electron Agric* (2019) 156:84–95. doi:10.1016/j.compag.2018.10.040

94. Jeon H, Zhu H. Evaluation of real-time stereo vision-controlled variable rate sprayer performance in grapevine shoot detections and spray application. *Smart Agric Technology* (2025) 12:101101. doi:10.1016/j.atech.2025.101101

95. Zhang J, Chen Q, Zhou H, Zhang C, Jiang X, Lv X. CFD analysis and RSM-based design optimization of axial air-assisted sprayer deflectors for orchards. *Crop Prot* (2024) 184:106794. doi:10.1016/j.cropro.2024.106794

96. Song K, Liu J, He P, Zhang Q. 3D printing graphene lattice enabled smart silicate composites with piezoresistive and thermoelectric effects. *Carbon* (2025) 234:120026. doi:10.1016/j.carbon.2025.120026

97. Sovetova M, Kaiser CJ. Thermal and energy efficiency in 3D-printed buildings: review of geometric design, materials and printing processes. *Energy and Buildings* (2024) 323:114731. doi:10.1016/j.enbuild.2024.114731

98. Khan SA, Koç M. Advancing electrolyzer design through additive manufacturing: a review on 3D printing in hydrogen electrolysis. *Int J Hydrogen Energ* (2025) 174:151240. doi:10.1016/j.ijhydene.2025.151240